

PACS numbers: 42.55.Wd; 42.60.Da; 42.60.Mi
DOI: 10.1070/QE2014v044n01ABEH015281

Narrow-band erbium-doped fibre linear–ring laser

A.A. Kolegov, G.S. Sofienko, L.A. Minashina, A.V. Bochkov

Abstract. **We have demonstrated a narrow-band linear–ring fibre laser with an output power of 15 mW at a wavelength of 1.55 μm and an emission bandwidth less than 5 kHz. The laser frequency is stabilised by an unpumped active fibre section and fibre Bragg grating. The fibre laser operates in a travelling wave mode, which allows the spatial hole burning effect to be avoided. At a certain pump power level, the laser switches from continuous mode to repetitive-pulse operation, corresponding to relaxation oscillations.**

Keywords: *narrow-band fibre laser, linear–ring scheme, active fibre, fibre Bragg grating, relaxation oscillations.*

1. Introduction

Narrow-band fibre lasers are widely used in applications such as coherent optical sensors, high-resolution spectrometers, light sources in precision physical experiments and lidars. In particular, cw lasers emitting at 1.55 μm with an emission band narrower than 20 kHz are attractive for photonic Doppler velocimetry (PDV) interferometric systems.

One way to produce narrow-band fibre lasers is to use unidirectional ring cavities [1–6]. This approach ensures narrow-band lasing because there is no spatial hole burning effect. To obtain a spectrum of the order of several kilohertz in width or even narrower, use is commonly made of intracavity filters (such as narrow-band Fabry–Perot filters [7] and phase-shifted fibre Bragg gratings [6]). The simplest, and effective, way of narrowing a spectrum and improving emission stability is by using an unpumped active fibre section, which, in combination with a Bragg grating, forms a dynamic narrow-band filter with a transmission bandwidth in the order of several tens of megahertz [2, 4, 5]. Thus, a narrow-band laser can be made using a linear–ring scheme, which is often employed to control radiation parameters in designing pulsed [8, 9] and cw [2–5] lasers.

In this paper, we report a narrow-band cw linear–ring fibre laser emitting at a wavelength $\lambda = 1.55$ μm for PDV (MPDV) systems. The laser frequency is stabilised by a fibre Bragg grating and unpumped active fibre.

A.A. Kolegov, G.S. Sofienko, L.A. Minashina, A.V. Bochkov Russian Federal Nuclear Center–Zababakhin All-Russia Research Institute of Technical Physics, ul. Vasil'eva 13, 456770 Snezhinsk, Chelyabinsk region, Russia; e-mail: albatrosing@yandex.ru, bavsnz@yandex.ru

Received 13 July 2013; revision received 23 November 2013
Kvantovaya Elektronika **44** (1) 13–16 (2014)
Translated by O.M. Tsarev

2. Laser configuration

Figure 1 shows the ring laser configuration. The active section of the cavity is made of a 0.6-m length of erbium-doped fibre (Russian Federal Nuclear Center–Zababakhin All-Russia Research Institute of Technical Physics). The mode field diameter of the active fibre is 9.0 ± 0.5 μm (at $\lambda = 1.31$ μm) and its numerical aperture is NA = 0.13 ± 0.01. Its cladding comprises two coatings: an inner coating (SIEL 159-305, NA = 0.42) and a protective strengthening coating (DeSolite DS-2015). The absorption in the active fibre is 61 dB m^{-1} at $\lambda = 0.98$ μm and 148 dB m^{-1} at $\lambda = 1.53$ μm. The average erbium, aluminium and germanium concentrations are 0.63 wt %, 1.66 wt % and 0.07 wt %, respectively. The ion concentrations were evaluated using a Cameca SX100 electron probe X-ray microanalyser at the Zavaritsky Institute of Geology and Geochemistry, Ural Branch, Russian Academy of Sciences. The active fibre was pumped through a Thorlabs WD202A wavelength division multiplexer by a Thorlabs PL980P330J single-mode wavelength-stabilised (975 nm) laser diode with an output power of up to 330 mW. An Opto-Link polarisation-maintaining circulator was used to ensure unidirectional operation of the scheme and reduce interaction between polarisation modes. The linear part of the cavity comprised an unpumped active fibre section and a high-reflectivity fibre Bragg grating (FBG) in SMF-28 fibre with an aperture and core diameter matched to those of the active fibre. The unpumped fibre was used as a saturable absorber in which two counterpropagating waves formed a narrow-band dynamic absorption coefficient grating, which allowed longi-

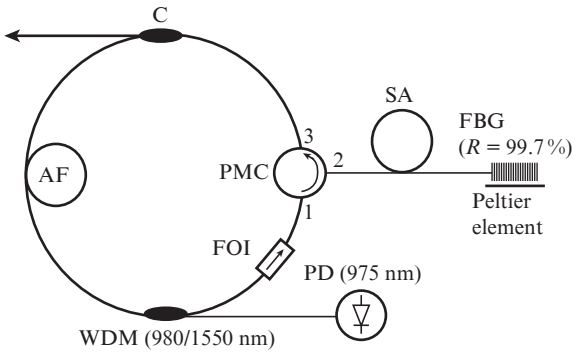

Figure 1. Fibre ring laser configuration: (AF) erbium-doped active fibre, (SA) saturable absorber (unpumped erbium-doped fibre), (PD) pump diode, (FOI) fibre-optic isolator, (WDM) wavelength division multiplexer, (PMC) polarisation-maintaining circulator, (FBG) fibre Bragg grating with a reflectance $R = 99.7\%$, (C) coupler.

tudinal modes to be effectively separated out and filtered off [10–12].

The bandwidth of such a filter is typically several tens of megahertz and depends on fibre length (determined by the doping level), and its resonance frequency corresponds to the laser wavelength. In addition, such an absorber ensures short-term laser wavelength stabilisation. The laser under consideration used a 6-cm-long saturable absorber containing 0.63 wt % erbium, which ensured a good relationship between the output power level and stability. The laser beam was out-coupled by a 1×2 coupler with a splitting ratio of 50:50. A Peltier element was used to tune the laser wavelength and thermally stabilise the Bragg grating. The total cavity length was about 6 m, and the length of the active section was 0.6 m.

3. Parameters of the laser and its components

Figure 2 shows the cw laser output power as a function of pump power. It is seen that the near-threshold behaviour of the output power depends on whether the pump power increases or decreases. The lasing threshold is 130 and 105 mW for increasing and decreasing pump power. This hysteretic behaviour is caused by the effect of the saturable absorber [5]. The slope efficiency of the laser is about 5%. This low efficiency may be the result of ion clustering, which considerably reduces the gain performance of heavily erbium-doped fibres, as shown by Plotskii et al. [13]. The highest laser output power is ~16 mW (at a pump power $P_p \approx 315$ mW). At $P_p = 320$ mW, the laser switches to repetitive-pulse operation. Figure 3 shows an oscilloscope trace of the signal power in this mode (measured with a PD-24-03 photodiode).

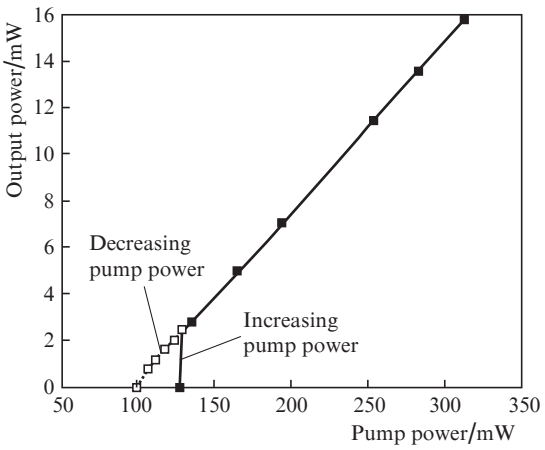

Figure 2. Laser output power as a function of pump power.

The ring part of the cavity is 6 m long, and its linear part is 1 m long, which corresponds to a fundamental pulse repetition rate of 25 MHz (pulse repetition time, 40 ns). It is seen in Fig. 3, however, that the actual pulse repetition rate is about 50 kHz (pulse repetition time, ~20 μs). The characteristics and shape of the signals in Fig. 3 correspond to relaxation oscillations [14–17]. Analysis of studies concerned with fibre laser dynamics suggests that such oscillations may originate from low-frequency pump modulation [14–16] or from injection of a signal whose wavelength falls within the gain band of the active fibre. Bolotskii and Petrov [17] described the synchronisation of relaxation oscillations in a ring fibre laser at a

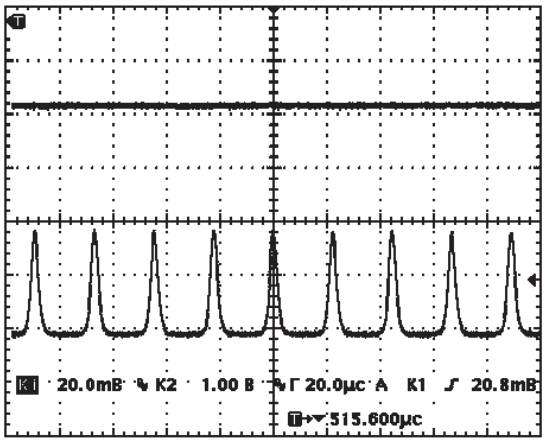

Figure 3. Oscilloscope trace illustrating the repetitive-pulse operation of the ring laser.

wavelength of 1.55 μm via the injection of external repetitive pulses from a semiconductor laser whose wavelength fell within the gain band of Yb–Er codoped fibre. Samson et al. [18] assume that relaxation oscillations may result from active-ion clustering. Ma et al. [19] presented a theoretical description of relaxation oscillations using analysis of luminescence.

One assumption as to the origin of the relaxation oscillations in the laser under consideration is that the laser light (the luminescence of the active fibre section) is reflected from high-loss fusion splices or fusion splices between mismatched fibres. One such splice is between the SMF-28 standard single-mode fibre and the polarisation-maintaining fibre of the circulator. Because of the geometry mismatch between these fibres, some of the light may be reflected. The estimated fraction of the power reflected in such geometry is [20]

$$k = 0.04\left(1 - \frac{P_0}{P_i}\right) = 0.04\left[1 - \frac{4r_0^2\rho_s^2}{(r_0^2 + \rho_s^2)^2}\right] \approx 0.003.$$

Here, P_0 is the power of the fundamental mode; P_i is the transmitted power; r_0 is the fibre core radius; and ρ_s is the mode spot radius.

For a laser signal in the milliwatt range, the reflected power is several microwatts, which is sufficient for the excitation of relaxation oscillations [16]. To verify this assumption, a fibre-optic isolator was fusion-spliced between the wavelength division multiplexer and polarisation-maintaining circulator (Fig. 1) to introduce losses through possible reflection from the fusion splice between the SMF-28 and circulator fibres. This allowed us to obtain 15 mW of output power in single-mode continuous operation at a pump power of 300 mW in the configuration under examination. With no isolator, the output power (without relaxation oscillations) reached 8 mW.

Figure 4 shows the laser output spectrum, measured using a Yokogawa AQ6370C spectrum analyser with a resolving power of 0.02 nm. The centre wavelength of the laser is 1550.1 nm, and the emission bandwidth is determined by the resolving power of the spectrum analyser.

To tune and stabilise the centre wavelength of the laser, the FBG was mounted on a Peltier element. Figure 5 shows the laser wavelength as a function of grating temperature. It is seen that the temperature coefficient of the laser wavelength is approximately 0.01 nm K^{-1}. Wavelength tunability makes the

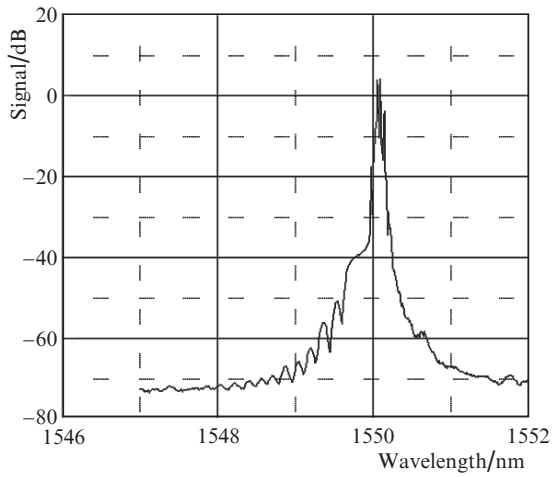

Figure 4. Emission spectrum of the laser.

proposed laser attractive for application in MPDV interferometric systems, which require multichannel lasers with a 3-GHz frequency difference (about 0.02 nm) between adjacent channels.

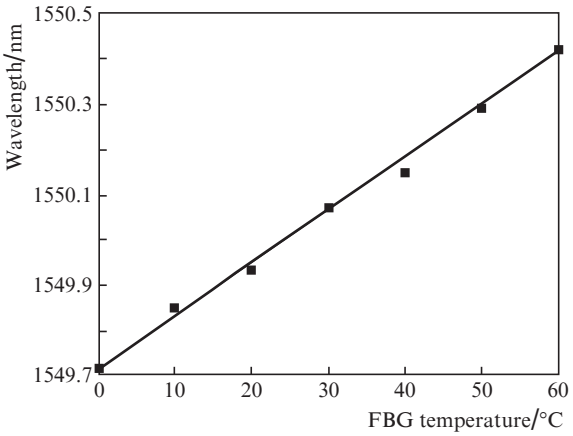

Figure 5. Laser wavelength as a function of fibre Bragg grating temperature.

The output spectrum of the narrow-band laser was measured using a technique reported by Trikshev et al. [21], who utilised a fibre ring interferometer to measure a laser emission spectrum. Such an interferometer is rather easy to make and allows relatively short delay lines (less than 2 km) to be used to measure laser emission bandwidths in the kilohertz range. Figure 6 shows the interference signal of a ring interferometer with a free spectral range of 236 kHz and response function of 5 kHz.

The spectral bandwidth obtained was about 5 kHz, which corresponded to the response function of the interferometer. Thus, we are led to conclude that the emission bandwidth of the proposed laser is within 5 kHz.

4. Conclusions

We have demonstrated a narrow-band ring laser emitting at a wavelength of 1550.1 nm with an emission bandwidth less

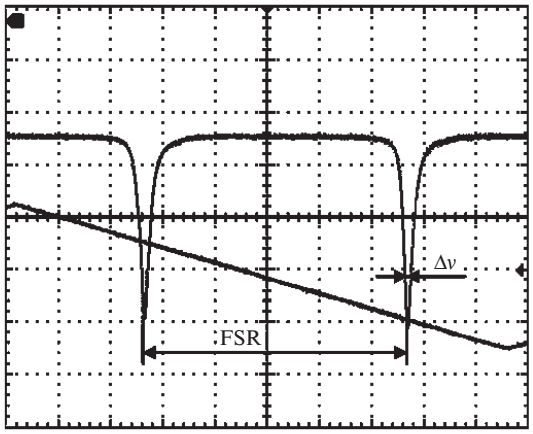

Figure 6. Interference signal of a ring interferometer with a free spectral range FSR = 235 kHz; $\Delta\nu$ is the spectral bandwidth.

than 5 kHz. The output power of the laser in single-frequency stable mode was ~15 mW at a pump power of 300 mW. At an average erbium concentration of 0.63 wt %, the active components of the laser were rather short: gain medium, 0.6 m; saturable absorber, 0.06 m. The centre wavelength of the laser can be tuned by varying the temperature of the fibre Bragg grating, with a temperature coefficient of about 0.01 nm K^{-1}.

The present results suggest that the laser can be used as a narrow-band source in PDV (MPDV) interferometric systems and other applications where a large coherence length is needed.

References

1. Cowle G.J., Payne D.N., Reid D. *Electron. Lett*., **3**, 229 (1991).
2. Cheng Y., Kringlebotn J.T., Loh W.H., Laming R.I., Payne D.N. *Opt. Lett*., **8**, 875 (1995).
3. Young J., Myong-Wook K., Bong K., Jyung L., Sang K., Sang C. *CLEO Pacific Rim'99*, **TuB4**, 23 (1999).
4. Song Y.W., Havstad S.A., Starodubov D., Xie Y., Willner A.E., Feinberg J. *IEEE Photonics Technol. Lett*., **11**, 1167 (2001).
5. Pan O., Yudong J., Bin C., Chunxi Z., Shuling H., Di F. *Chin. Opt. Lett*., **11**, 845 (2008).
6. Cheng X.P., Tse C.H., Shum P., Wu R.F., Tang M., Tan W.C., Zhang J. *J. Lightwave Technol*., **8**, 945 (2008).
7. Park N., Dawson J.W., Vahala K.J., Miller C. *Appl. Phys. Lett*., **59**, 2369 (1991).
8. Nyushkov B.N., Denisov V.I., Kobtsev S.M., Pivtsov V.S., Kolyada N.A., Ivanenko A.V., Turitsyn S.K. *Laser Phys. Lett*., **7**, 661 (2010).
9. Denisov V.I., Ivanenko A.V., Nyushkov B.N., Pivtsov V.S. *Kvantovaya Elektron*., **38**, 801 (2008) [*Quantum Electron*., **38**, 801 (2008)].
10. Chen H.X., Babin F., Leblanc M., Schinn G.W. *IEEE Photonics Technol. Lett*., **15**, 185 (2003).
11. Liu J., Yao J.P., Yao J., Yeap T.H. *IEEE Photonics Technol. Lett*., **16**, 1020 (2004).
12. Paschotta R., Nilsson J., Reekie L., Tropper A.C., Hanna D.C. *Opt. Lett*., **22**, 40 (1997).
13. Plotskii A.Yu., Kurkov A.S., Yashkov M.Yu., Bubnov M.M., Likhachev M.E., Sysolyatin A.A., Gur'yanov A.N., Dianov E.M. *Kvantovaya Elektron*., **35**, 559 (2005) [*Quantum Electron*., **35**, 559 (2005)].
14. Okhotnikov O.G., Salsedo J.R. *IEEE Photonics Technol. Lett.*, **3**, 367 (1994).
15. Lacot E., Stoeckel F., Chenevier M. *Phys. Rev. A*, **49**, 3997 (1994).
16. Ionov S.I., Barnes W.L., Jedrzejewski K.P. *Electron. Lett*., **21**, 1958 (1991).

17. Bolotskii V.I., Petrov M.P. *Pis'ma Zh. Tekh. Fiz*., **2**, 24 (1999).
18. Samson B.N., Loh W.H., de Sandro J.P. *Opt. Lett*., **23**, 1763 (1997).
19. Ma L., Hu Z., Liang X., Meng Z., Hu Y. *Appl. Opt*., **10**, 1979 (2010).
20. Snyder A.W., Love J.D. *Optical Waveguide Theory* (London: Chapman and Hall, 1983; Moscow: Radio i Svyaz', 1987).
21. Trikshev A.I., Kurkov A.S., Tsvetkov V.B., Pyrkov Yu.N., Paramonov V.N. *Kvantovaya Elektron*., **41**, 656 (2011) [*Quantum Electron*., **41**, 656 (2011)].